

1 **HCl-doping of V/TiO₂-based catalysts reveals the promotion of NH₃-**
2 **SCR and the rate limiting role of NO oxidative activation**

3
4
5 Aldo Lanza^a, Lei Zheng^{a,b}, Roberto Matarrese^a, Luca Lietti^a, Jan-Dierk Grunwaldt^b, Silvia Alcove
6 Clave^c, Jillian Collier^c, Alessandra Beretta^{a,*}

7
8 *^aLaboratory of Catalysis and Catalytic Processes, Dipartimento di Energia, Politecnico di Milano,*
9 *via La Masa 34, 20156 Milano, Italy*

10 *^bInstitute for Chemical Technology and Polymer Chemistry, Karlsruhe Institute of Technology, 76131*
11 *Karlsruhe, Germany*

12 *^cJohnson Matthey Technology Centre, Blounts Ct Rd, Sonning Common, Reading RG4 9NH, United*
13 *Kingdom*

14
15
16
17
18
19
20
21
22
23
24
25
26
27
28
29 *Key-words:* NH₃-SCR, HCl, V₂O₅-MoO₃/TiO₂, NO activation, transient kinetic experiments,
30 *operando FT-IR*

31
32
33
34

35 **Abstract**

36 NH₃-SCR is the best available technology for NO_x abatement from power plant, incinerators,
37 gasifiers, and a well-established technology for on board NO_x emission control; in the last 40 years,
38 the reaction mechanism and kinetics have been deeply investigated, but the understanding of the
39 nature of surface intermediates and rate determining steps is still object of a lively discussion. A major
40 factor, though, has been largely neglected in the scientific literature, that is the presence of HCl in the
41 flue gases generated by coal, biomass and plastics. In this work, the effect of HCl on NH₃-SCR over
42 V₂O₅ catalysts was investigated through combined kinetic analysis and operando FTIR.
43 Unexpectedly, after HCl-doping, the catalyst intrinsic activity of a commercial catalyst increased by
44 a factor of 5. Besides, it was found that while the NH₃ surface coverage is little affected by HCl-
45 doping, the chemisorption capacity of NO+O₂ undergoes a remarkable promotion that scales with the
46 promotion of the reaction rate. The HCl-effect provided thus an indirect but unambiguous piece of
47 evidence that NO-activation by an O-species is a key rate controlling step of NH₃-SCR.

48

49

50

51

52

53

54

55

56

57

58

59

60

61 **1. Introduction**

62 NH₃-SCR (Selective Catalytic Reduction) is the best available technology for the abatement
63 of nitrogen oxides emitted by power plants, stationary and marine diesel engines and other energy
64 conversion systems based on the combustion or gasification of coal, biomass, organic waste and
65 plastics [1-8]. The technology is now being deployed also in light and heavy-duty diesel vehicles.

66 Ternary V₂O₅-MoO₃(WO₃)/ TiO₂ formulations represent the catalysts of choice in stationary
67 applications but their use in on-board deNO_x units is also widespread in Asian countries, such as
68 China. Despite an over 40-years-long history of studies, the mechanism and kinetics of NH₃-SCR on
69 V are still discussed and fertile soil of new findings [9-19]. Remarkably, a major factor, relevant in
70 stationary applications, has been largely neglected (with very few exceptions [20-22, 26]) in the
71 scientific literature, that is the presence of HCl in the flue gases. Novel studies from Perez-Ramirez's
72 group and others have shown the tendency of several metal oxides, including TiO₂, and redox oxides
73 like V₂O₅, to combine with HCl; which suggests possible implications for the SCR reaction [23-25].
74 Recently, the effect of HCl on the SCR activity of a MnCe catalyst was studied and a permanent
75 deactivation was found due to volatilization of Mn [26]. However, commercial V-based SCR catalysts
76 are designed to operate stably under HCl-containing flue gases.

77 The presence of HCl in the flue gases and its interaction with the V-based catalysts is
78 unanimously recognized as the key behind the chemistry of the so-called mercury oxidation on SCR
79 catalysts, a reaction of great interest because of the growing concern and emerging stringent
80 regulations on Hg emissions from stationary power plants; across the SCR reactor, mercury is subject
81 to combined oxidation and chlorination, highly desirable since the product HgCl₂ is more easily
82 removed from the flue gases by means of conventional wet scrubbers downstream from the SCR unit.
83 Recent DFT and kinetic studies have proposed the formation of chlorinated V-species [27-33].
84 Experience and theory thus confirm the ability of V-catalysts to bond and release Cl species from
85 gas-phase HCl but what is the effect of V-HCl interaction on the chemistry and kinetics of NH₃-SCR
86 is still unknown. Within a more extended kinetic investigation on Hg/HCl/O₂/NO/ NH₃ reacting

87 systems, we were driven into this long-overlooked aspect. Experiments were performed over a
88 proprietary V₂O₅/MoO₃/TiO₂ catalyst and a model V/TiO₂ catalyst where HCl-doping was obtained
89 by pre-impregnation. Transient activity tests and operando FT-IR experiments provided novel pieces
90 of evidence on the kinetics of NH₃-SCR. In particular, the breakthrough evidence on the kinetic
91 relevance of NO oxidative activation was clearly obtained.

92 The interaction of NO_x with V-sites has been discussed in the broad literature of standard and
93 fast NH₃-SCR in close relation with the redox nature of the catalytic cycle; a debate is still open.
94 Koebel et al. first showed that the powerful oxidizing property of NO₂ enhanced the kinetics of the
95 oxidation step of the redox cycle (V⁴⁺ → V⁵⁺) and could explain the promoted kinetics of the fast SCR
96 [34-37]. Similarly, surface nitrite/nitrate intermediates have been proposed to behave as enhancers of
97 V⁴⁺ re-oxidation in the standard SCR by Arnarson et al. (based on DFT calculations) and by Beretta
98 et al. (based on kinetic evidence) [38,9]. Concerning the reduction step, it is well known that the
99 seminal studies by Ramis et al. [1,4,13] and Topsøe et al. [14,15,39] have proposed (based on
100 spectroscopic results) the kinetic relevance of NH₃ partial oxidation to a surface N²⁻ species. Instead,
101 Tronconi and co-workers have proposed the rate controlling role of NO adsorption over an oxidized
102 site with formation of a surface N³⁺ species, able to rapidly react with adsorbed NH₃ and produce N₂,
103 leaving a reduced site V⁴⁺ [40]. Recent studies investigated the promotion of low-temperature SCR
104 by using Ce-modified V-based catalysts and have addressed the role of surface NO_x and nitrates
105 (whose storage is largely promoted by CeO₂ sites) in the reaction mechanism [41- 48]. Brückner and
106 coworkers [41] found that Ce_{1-x}Ti_xO₂ supports were as active in NH₃-SCR, as in the formation of
107 nitrates from gaseous NO+O₂, however the involvement of adsorbed NO* intermediates was
108 excluded when V was added (since no nitrate formation was observed over V-containing catalysts at
109 200°C). Instead, Li and coworkers [42, 43] confirmed the promoting effect of the VO_x-Ce interaction,
110 associating it to the largely favored formation of surface NO_x species.

111 The present work aims at contributing to the presently open debate on the kinetics of NH₃-
112 SCR on V-based catalysts, whose deep comprehension can lead to new formulations able to enhance
113 the low-temperature NO_x conversion.

114

115 **2. Materials and methods**

116 **2.1 Experimental**

117 *Catalyst samples* - SCR experiments were performed over a proprietary Johnson Matthey
118 V₂O₅/MoO₃/TiO₂ commercial catalyst developed for coal-fired power plants and combined biomass-
119 coal-fired power plants; the same catalyst formulation was the object of previous studies [9, 33]. Prior
120 to testing, the catalyst was pre-treated in flowing air at 450°C in a packed-bed reactor.

121 HCl-doping was obtained by impregnation with an aqueous solution of HCl (IWI method,
122 details in Supplementary Material). After drying at 110°C, the concentration of HCl deposited by this
123 methodology was estimated by ICP analysis at 35-40 μmol/g_{cat}.

124 Both doped and undoped catalysts were sieved (140-200 mesh) to obtain powders for the
125 kinetic investigations in a lab-scale packed-bed reactor.

126 A 2%V/TiO₂ model catalyst was also used, as such and impregnated with HCl with ratio
127 V/HCl=1.

128 *Lab-scale apparatus for the kinetic investigations* – The SCR activity and temperature
129 programmed tests were performed in a micro fixed-bed reactor, consisting of a quartz tube (with 9
130 mm ID). The catalytic bed was diluted with quartz particles (140-200 mesh). Above the catalytic bed
131 an additional bed of inert quartz granules (10-14 mesh) was loaded to obtain uniform flow distribution
132 and preheating of the inlet stream. The reactor was placed in an electric-oven and the temperature
133 was controlled by a type K thermocouple placed in the catalytic bed. A Pfeiffer Vacuum ThermoStar
134 mass spectrometer was connected to the exhaust gases to continuously analyze the products.

135 NH₃-SCR activity tests were performed over the HCl-VMoTi catalyst by an initial
136 adsorption/stabilization phase with flowing NH₃= 320 ppm, NO= 300 ppm and O₂= 3% in He at

137 150°C, followed by a temperature ramp from 150 to 400°C (5°C/min). After 3 hours of hold at 400°C,
138 the reactor was cooled down and a second run was then repeated over the same sample with the same
139 procedure.

140 The NO-TPSR were performed over HCl-VMoTi catalyst and the reference VMoTi catalyst
141 after NH₃ pre-adsorption at 100°C (NH₃=500 ppm, 90 minutes). A ramp under NO=100
142 ppm+O₂=1000 ppm was then run from 100°C to 450°C (5°C/min). A second run was repeated on
143 each sample.

144 The NO+O₂ adsorption/desorption tests were performed over HCl-VMoTi and over the
145 reference VMoTi catalyst. After the initial storage phase under flowing NO=100 ppm and O₂=1000
146 ppm in He at 100 °C of 2 hours, a temperature ramp was then run from 100 to 400°C (5°C/min).

147 Steady state NH₃-SCR activity tests were performed over the HCl-doped and undoped VMoTi
148 commercial sample and binary 2%V/TiO₂ model catalyst with flowing NH₃= 320 ppm, NO= 300
149 ppm and O₂= 3% in He.

150 Additional details on the procedure and operating conditions of each experiment (catalyst
151 load, bed dilution, total flow rate) are given in the Supplementary Material.

152 ***Operando FT-IR tests***– The NO_x and NH₃ storage capacity was investigated over the HCl
153 treated 2%V/Ti catalyst and over the reference 2%V/Ti catalyst. The catalysts in the form of self-
154 supported disks of ca. 15 mg were placed in a heated IR reactor cell (ISRI Infrared Reactor, Granger,
155 IN, USA) working under flowing gases. NO and NH₃ adsorption were carried out at ambient
156 temperature with NO (1000 ppm) in He + O₂ (3%, v/v) or 500 ppm of NH₃/He for 30 minutes,
157 respectively. Additional details on the experimental apparatus and procedures are reported in the
158 Supplementary Material and elsewhere [49].

159 **2.2 Packed-bed reactor model**

160 A steady state model of the plug flow micro-reactor has been reported elsewhere [9] and
161 therein applied to the development of redox kinetics of NH₃-SCR, accounting for several
162 compositional effects. The model consists of the differential mass balances of the reacting species

163 and accounts for the possible contribution of intra-porous mass transfer limitations. In this work, the
164 same model was used as a simple tool for data analysis and estimation of the intrinsic activity. At this
165 scope, the simplifying assumption of pseudo-first order kinetics was done, such that the model
166 reduces to the mass balance of the species NO. All the details of the model and its use for the estimate
167 of the kinetic constants are reported in the Supplementary Material.

168

169 **3. Results**

170 *SCR activity tests* - Figure 1 reports the results of two consecutive dynamic NH₃-SCR
171 experiments over a HCl-impregnated sample.

172 [Figure 1]

173 In the first run, the reaction onset was observed at about 150°C; NO conversion grew with
174 temperature with an activation energy of 92 kJ/mol (Figure S1) and turnover rates by far higher than
175 those of the undoped catalyst. Above 275°C, NO conversion grew only moderately, then flattened at
176 about 95% and finally decreased down to 83% during the 3-hours hold at 400°C. The high
177 temperature loss of activity can be easily explained by the loss of HCl via desorption in the gas phase:
178 this was indeed confirmed by a TPD experiment carried out over the HCl-doped VMoTi catalyst in
179 flowing 0.5% O₂ in He (Figure S2), showing the release of HCl above 200°C.

180 Then, after cooling the catalyst, a second run was started with the same flow conditions: the
181 conversion curve appeared shifted by about 50°C, and is representative of the behavior of a HCl-free
182 catalyst sample. In fact at 400°C the same conversion of 83% was observed during the second ramp.

183 The experiment revealed the formidable promotion of the reaction by HCl addition; at 225°C,
184 the intrinsic rate constant increased by a factor of 5 as shown by the Arrhenius plot of pseudo-first
185 order kinetic constants in Figure S1.

186 Additional experiments were performed to follow the loss in the catalyst activity at high
187 temperature due to the loss of HCl. Starting from the HCl-doped VMoTi catalyst at 350°C, Figure S3
188 shows that the NO conversion decreases from over 90% down to about 70% in 4 hours on stream

189 (blue squares), eventually reaching the activity of the fresh catalyst (red squares). Then, upon
190 decreasing the temperature of the HCl-doped VMoTi catalyst, the reactivity of the doped and undoped
191 samples are superimposed.

192

193 ***NO+O₂-TPSR tests*** - NO+O₂-TPSR (Temperature Programmed Surface Reaction) with
194 flowing NO and O₂ in He after NH₃ pre-adsorption at 100°C were also performed on both the HCl-
195 doped catalyst and the undoped catalyst. The whole procedure is described in detail in the
196 Supplementary Material. This kind of experiments allows to identify the onset of the reaction and
197 quantify the amount of reacted NH₃ from the surface. Therefore, the comparison between the NO+O₂-
198 TPSR tests on catalysts with and without HCl allows to measure simultaneously the effect of HCl on
199 both the reaction rate and the NH₃-storage capacity. The results are reported in synthetic form in
200 Figure 2 and in detailed form in Figure S4.

201

[Figure 2]

202 Both the undoped and the HCl-doped catalysts were subject to two consecutive experiments;
203 Figure 2 reports for brevity the results of the first run over the undoped catalysts (the second ramp
204 was identical), and the two consecutive runs over the HCl-doped catalyst. Over both doped and
205 undoped catalysts, NH₃ desorption occurred as soon as the temperature ramp started, the
206 concentration was maximum at about 250°C and then decreased rapidly with increasing temperature
207 (Figure S4). Concerning NO consumption and N₂ formation (Figure S5), these started around 150°C
208 in the first ramp over the HCl-doped catalyst: NO conversion grew rapidly, peaked at 70% at about
209 270°C, then extinguished as soon as the NH₃ coverage dropped. In the repeated experiment (second
210 ramp in Figure 2, black curve), the onset of NO conversion was observed at 200°C with significantly
211 lower initial rate; the overall consumption was also significantly lower. The comparison reported in
212 Figure 2 (black line vs red line) reveals that these features are the same as those of the undoped
213 catalyst, a further confirmation that the high temperature desorption of HCl leaves unchanged the
214 surface of the catalyst and that the presence of HCl produced the important promotion of the reaction.

215 The integral consumption of NO amounted to 105 $\mu\text{mol/g}_{\text{cat}}$ over the HCl-doped catalyst and
216 51 $\mu\text{mol/g}_{\text{cat}}$ over the undoped catalyst; by considering also the overall desorption of NH_3 during the
217 experiments, it was estimated that NH_3 coverage amounted to about 270 $\mu\text{mol/g}_{\text{cat}}$ (at 100°C) on both
218 HCl-doped and undoped catalyst. Which cannot explain the dramatic promotion of the reaction rate.

219 A simple quantitative analysis was performed over the low-temperature range of the TPSR
220 curves (where the absence of any stoichiometric limitation by ammonia can be assumed). Pseudo-
221 first order kinetic constants were estimated for the undoped and the HCl-doped catalyst, as detailed
222 in the Supplementary Material (Figure S6); the analysis confirmed the estimate of an activation
223 energy of 92 kJ/mol in the range 150-250°C and a promotion factor by over 550% after HCl doping.

224 The effect of HCl doping was investigated also on a binary model 2% V/TiO₂ catalyst.
225 Reference steady-state NH_3 -SCR experiments were first performed over the undoped catalyst under
226 similar operating conditions as those used for the ternary commercial catalyst; a remarkable increase
227 of the intrinsic activity was found (compared with the commercial catalyst), as expected for the large
228 V-content. The temperature range of the experiments was thus limited to an upper value of 280°C.
229 The binary catalyst was also impregnated with HCl and experiments were repeated over the HCl-
230 doped catalyst; a remarkable increase of the activity was found, as documented in figure S7.

231 It was thus concluded that the interaction of HCl with the V-TiO₂ system is the key behind
232 the observed performance of the ternary catalyst, despite the complex formulation of the commercial
233 catalyst, that, together with the MoO₃ component typically includes several additives that convey
234 structural and mechanical stability.

235 *NO_x storage experiments* - To further study the origin of the paramount effect on the DeNO_x
236 activity, pieces of evidence on the effect of HCl on the adsorption/activation of reactants were
237 searched by dedicated experiments in the packed bed reactor (commercial catalyst) and in an
238 operando FT-IR cell (model catalyst).

239 Figure 3 reports the results of experiments of NO+O₂ adsorption at 100°C over the ternary
240 commercial catalyst, followed by temperature ramp (under flowing NO + O₂). The procedure is
241 described in detail in the Supplementary Material.

242 [Figure 3]

243 Negligible adsorption and desorption of NO were observed over the undoped catalyst at
244 100°C (red line in Figure 3). Indeed, the negligible NO adsorption capacity of V-catalysts is well
245 known and is the evidence behind the kinetic formalism of the Eley-Rideal rate expression, commonly
246 adopted to describe the process [41, 50-52]. Instead, surprisingly, a significant NO peak was observed
247 after the adsorption phase for the HCl-doped catalyst. NO desorption started at 150°C, peaked at
248 about 200°C and extinguished at about 230°C. The temperature range involved in the desorption are
249 the clear evidence of the existence of chemisorbed NO species and since the experiment was
250 performed in the presence of O₂, we herein infer that the chemisorbing site was a surface O* or OH*
251 species. The experiment thus reveals that more abundant adsorbed NO species were formed after the
252 HCl-doping.

253 Further support was obtained by operando FT-IR experiments over a model 2% V/TiO₂
254 catalyst with and without HCl-doping. Experiments were performed over the binary catalyst in order
255 to maximize the sensitivity. After a mild drying treatment in O₂/He flow, a NO+O₂ in He stream was
256 admitted to the IR cell. Figure 4 shows the evolution of the spectra collected during 30 minutes from
257 the reactant inlet.

258 [Figure 4]

259 Panel (a) refers to the undoped catalyst, while panel (b) refers to the HCl-doped 2% V/TiO₂
260 sample. In both cases the progressive accumulation of NO_x surface species occurred. According to
261 the literature the main formation of different kind of surface nitrates (i.e. bridging, bidentate and
262 monodentate nitrates) was observed in the 1650-1450 and 1300-1200 cm⁻¹ regions [13,53,54].
263 Moreover, the presence of minor amounts of surface nitrites with both nitro and nitrito structures
264 cannot be excluded because of their strong overlapping with nitrates. However, the intensity of signals

265 obtained over the HCl-doped sample was significantly higher than that of the undoped catalyst. The
266 perturbation of the fundamental vanadyl (at about 1028 cm^{-1}) and of the overtone (about 2045 cm^{-1} ,
267 see insert in the Figure) were significantly more intense over the chlorinated catalyst, in line with the
268 increased amounts of NO_x adsorbed [55,56].

269 NH_3 adsorption experiments were also performed in the FTIR apparatus; spectra were
270 collected during the first 30 minutes after injection of the NH_3 containing stream. As reported in
271 Figure S8, peaks representative of NH_3 adsorbed over Bronsted and Lewis acid sites were observed,
272 but no appreciable difference between the undoped and HCl-doped samples were visible. This
273 suggests that the surface acidity was not significantly modified by the presence of HCl.

274

275 **4. Discussion**

276 The bulk of data herein presented demonstrate a powerful promoting effect of HCl addition
277 on the SCR reaction. The overall coverage and strength of adsorption of NH_3 did not change
278 significantly after HCl doping; instead, an unexpected increase of the low temperature adsorption of
279 NO in the form of nitrates was observed over the HCl-doped catalyst. The stored nitrates decompose
280 upon heating, thus restoring gas-phase NO.

281 Notably, the same nitrate species are also formed over the undoped catalyst, but the storage is
282 exalted in the presence of HCl. We thus speculate that the NO adsorption and activation has a role in
283 the SCR reaction, and that the presence of HCl affects the NO interaction and reactivity with the
284 active V sites. It is interesting to observe that the formation of nitrates from gas phase NO and O_2 and
285 the reversible decomposition of nitrates to NO is the demonstration that nitrogen can travel through
286 a reversible pattern between N^{2+} to N^{5+} . Within this pattern, the true reactive species is formed, i.e.
287 an intermediate whose oxidation state suitably matches and balances the reduced state of nitrogen in
288 the ammonia-derived adsorbed species (an amide species with state N^{2-} according to the conclusions
289 of Topsoe [14,15,39] and Busca et al.[1,13] studies, or an adsorbed ammonia with state N^{3-} according

290 to Tronconi et al.[40]), although based on the present experiments we cannot speculate on the exact
291 nature of such intermediate.

292 The redox nature of the reaction cycle has been recently confirmed in the literature, using
293 operando characterization techniques, DFT, modeling and traditional experiments [9,38,52,57-60].
294 By means of dynamic experiments and time-resolved spectroscopic studies with isotopically labelled
295 molecules, Wachs and coworkers have further proposed the kinetic relevance of NH₃ activation [2,
296 61]. The experiments herein reported show instead the kinetic relevance of NO activation, which
297 conclusion is not necessarily contradictory with Wachs' proposal. In fact, also Wachs and coworkers
298 confirmed that NH₃ alone cannot be the reducing agent in NH₃-SCR, while the combined NO/NH₃
299 mixture shows a synergistic reducing effect, as clearly demonstrated also by Ferri et al. [52].

300 We can speculate that adsorbed HCl interacts with V=O, giving rise to the formation of highly
301 active Cl-V-OH sites as proposed by He et al. and Yang et al. [22,25]; such sites could favor the
302 adsorption of NO and its transformation into an oxidized species that boosts the low temperature SCR
303 activity. In the case of CeO₂-promoted VO_x catalysts, Hu et al. have identified such a species as
304 HONO [62]

305

306 **5. Conclusions**

307 This work reports the results of a focused experimental campaign, which demonstrated the
308 promoting effect of HCl doping on the DeNO_x performance of a commercial V/Mo/Ti catalyst.
309 Besides, it was found that HCl doping greatly enhances the adsorption of NO + O₂, while it increases
310 only moderately the NH₃-storage. Thus, indirectly, the HCl effect (by perturbing the reacting system)
311 also demonstrates that NO activation is truly kinetically limiting and passes through an oxidative
312 adsorption.

313 The implications of the present results may be very important, spanning from the
314 improvement of SCR catalysts formulations based on the concept that oxidative adsorption of NO is
315 needed, to the development of catalysts and processes for NO_x adsorption and release. Further

316 research is needed to identify the nature of the NO-adsorption site and of V-HCl interaction by the
317 combination of characterization, transient and steady state experiments.

318

319

320

321 **Notation**

322 $VMoTi = V_2O_5/MoO_3/TiO_2$ commercial catalyst

323 $HCl - VMoTi = HCl$ -doped $V_2O_5/MoO_3/TiO_2$ commercial catalyst

324 $HCl - 2\%V/Ti = HCl$ -doped 2%V/ TiO_2 binary model catalyst, nominal ratio V:HCl=1

325 $IWI =$ incipient wetness impregnation

326 $ID =$ internal diameter of the quartz tube reactor [mm]

327

328 **Acknowledgements**

329 A.L. acknowledges the financial contributions to his PhD scholarship from the Ministry of
330 University and Research (MUR) and the Energy for Motion project of Department of Energy,
331 Politecnico di Milano. L. Z. thanks the provision of a research travel grant by Karlsruhe House of
332 Young Scientist (KHYS). LL and RM gratefully acknowledge the contribution of Fondazione
333 Banca del Monte di Lombardia for the FTIR-operando set-up. The authors are thankful to the
334 colleagues prof. Enrico Tronconi, prof. Elisabetta Finocchio and prof. Guido Busca for insightful
335 discussion.

336

337 **References**

338 [1] G. Busca, L. Lietti, G. Ramis, F. Berti, Chemical and Mechanistic Aspects of the Selective
339 Catalytic Reduction of NO_x by Ammonia over Oxide Catalysts: A review. Appl. Catal. B Environ.
340 18 (1) (1998) 1-36.

341 [2] M. Zhu, J-K. Lai, M. E. Tumuluri, Z. Wu, I. E. Wachs, Reaction pathways and kinetics for
342 selective catalytic reduction (SCR) of acidic NO_x emissions from power plants with NH_3 , ACS Catal.
343 7 (12) (2017) 8358-8361.

344 [3] P. Forzatti, L. Lietti, E. Tronconi, Nitrogen Oxides Removal-Industrial, Encyclopedia of
345 Catalysis, John Wiley & Sons Inc. (2012).

- 346 [4] L. Lietti, I. Nova, G. Ramis, L. Dall'acqua, G. Busca, E. Giamello, P. Forzatti, F. Bregani,
347 Characterization and reactivity of V₂O₅-MoO₃/TiO₂ De-NO_x SCR Catalysts, *J. Catal.* 187 (1999) 419-
348 435.
- 349 [5] L. J. Alemany, L. Lietti, N. Ferlazzo, P. Forzatti, G. Busca, E. Giamello, F. Bregani, Reactivity
350 and Physicochemical Characterization of V₂O₅-WO₃/TiO₂ De-NO_x SCR Catalysts, *J. Catal.* 155 (1)
351 (1995) 117-130.
- 352 [6] J.-K. Lai, I. E. Wachs, A Perspective on the Selective Catalytic Reduction (SCR) of NO with NH₃
353 by Supported V₂O₅-WO₃/TiO₂ Catalysts. *ACS Catal.* 8 (7) (2018) 6537-6551.
- 354 [7] P. Forzatti, I. Nova, E. Tronconi, New "Enhanced NH₃-SCR" Reaction for NO_x Emission Control,
355 *Ind. Eng. Chem. Res.* 49 (21) (2010) 10386-10391.
- 356 [8] L. Zheng, M. Casapu, M. Stehle, O. Deutschmann, J.-D. Grunwaldt, Selective Catalytic Reduction
357 of NO_x with Ammonia and Hydrocarbon Oxidation Over V₂O₅-MoO₃/TiO₂ and V₂O₅-WO₃/TiO₂ SCR
358 Catalysts, *Top. Catal.* 62 (2019) 129-139
- 359 [9] A. Beretta, A. Lanza, L. Lietti, S. Alcove Clave, J. Collier, M. Nash, An investigation on the redox
360 kinetics of NH₃-SCR over a V/Mo/Ti catalyst: Evidence of a direct role of NO in the re-oxidation
361 step, *Chem. Eng. J.* 359 (2019) 88-98.
- 362 [10] C. Wang, C. Li, Y. Li, L. Huangfu, Z. Liu, S. Gao, J. Yu, Destructive Influence of Cement Dust
363 on the Structure and DeNO_x Performance of V-Based SCR Catalyst, *Ind. Eng. Chem. Res.* 58 (43)
364 (2019) 19847-19854.
- 365 [11] T. V. W. Janssens, H. Falsig, L. F. Lundegaard, P. N. R. Vennestrom, S. B. Rasmussen, P. G.
366 Moses, F. Giordanino, E. Borfecchia, K. A. Lomachenko, C. Lamberti, S. Bordiga, A. Godiksen, S.
367 Mossin, P. Beato, A Consistent Reaction Scheme for the Selective Catalytic Reduction of Nitrogen
368 Oxides with Ammonia, *ACS Catal.* 5 (5) (2015) 2832-2845.
- 369 [12] I. Nova, A. Beretta, G. Groppi, L. Lietti, E. Tronconi, P. Forzatti, Monolithic catalysts for NO_x
370 removal from Stationary Sources, *Structured Catalysts and Reactors* (2nd ed.), Taylor & Francis.
371 (2006) 171-214.
- 372 [13] G. Ramis, G. Busca, F. Bregani, P. Forzatti, Fourier transform-infrared study of the adsorption
373 and coadsorption of nitric oxide, nitrogen dioxide and ammonia on vanadia-titania and mechanism
374 of selective catalytic reduction, *Appl. Catal.* 64 (1990) 259-278.

- 375 [14] N.-Y. Topsoe, H. Topsoe, J. A. Dumesic, Vanadia/titania catalysts for selective catalytic
376 reduction (SCR) of nitric oxide by ammonia. I, *J. Catal.* 151 (1995) 226-240.
- 377 [15] J. A. Dumesic, N.-Y. Topsoe, H. Topsoe, Y. Chen, T. Slabiak, Kinetic of selective catalytic
378 reduction of nitric oxide by ammonia over vanadia/titania, *J. Catal.* 163 (1996) 409-417.
- 379 [16] I. Nova, C. Ciardelli, E. Tronconi, NH₃-SCR of NO over a V-based catalyst: low-T redox kinetics
380 with NH₃ inhibition, *AIChE J.* 52 (9) (2006) 3222-3233.
- 381 [17] L. Casagrande, L. Lietti, I. Nova, P. Forzatti, A. Baiker, SCR of NO by NH₃ over TiO₂-supported
382 V₂O₅-MoO₃ catalysts: reactivity and redox behavior, *Appl. Catal. B Environ.* 22 (1) (1999) 69-77.
- 383 [18] T. Yan, Q. Liu, S. Wang, G. Xu, M. Wu, J. Chen, J. Li, Promoter rather than Inhibitor:
384 Phosphorus Incorporation Accelerates the Activity of V₂O₅-WO₃/TiO₂ Catalyst for Selective
385 Catalytic Reduction of NO_x by NH₃, *ACS Catal.* 10 (2020) 2747-2753.
- 386 [19] N.R. Jaegers, J.K. Lai, Y. He, E. Walter, D.A. Dixon, M. Vasiliu, Y. Chen, C. Wang, M.Y. Hu,
387 K.T. Mueller, I.E. Wachs, Y. Wang, J.Z. Hu, Mechanism by which Tungsten Oxide Promotes the
388 Activity of Supported V₂O₅/TiO₂ Catalysts for NO_x Abatement: Structural Effects Revealed by
389 51V MAS NMR Spectroscopy, *Angew. Chemie - Int. Ed.* 58 (2019) 12609–12616.
- 390 [20] L. Lisi, G. Lasorella, G. Russo, Single and combined deactivating effect of alkali metals and HCl
391 on commercial SCR catalysts, *Appl. Catal. B Environ.* 50 (4) (2004) 251-258.
- 392 [21] Y. Hou, G. Cai, Z. Huang, X. Han, S. Guo, Effect of HCl on V₂O₅/AC catalyst for NO reduction
393 by NH₃ at low temperatures, *Chem. Eng. J.* 247 (2014) 59-65.
- 394 [22] Y. Yang, W. Xu, J. Wang, T. Zhu, New insight into simultaneous removal of NO and Hg⁰ on
395 CeO₂-modified V₂O₅/TiO₂ catalyst: A new modification strategy, *Fuel.* 249 (2019) 178-187.
- 396 [23] M. A.G. Hevia, A. P. Amrute, T. Schmidt, J. Pérez-Ramirez, Transient mechanistic study of the
397 gas-phase HCl oxidation to Cl₂ on bulk and supported RuO₂ catalysts, *J. Catal.* 276 (1) (2010) 141-
398 151.
- 399 [24] R. Liu, W. Xu, L. Tong, T. Zhu, Mechanism of Hg⁰ oxidation in the presence of HCl over a
400 commercial V₂O₅-WO₃/TiO₂ SCR catalyst, *J. Environ. Sci.* 36 (2015) 78-83.
- 401 [25] H. Sheng, Z. Jinsong, Z. Yanqun, L. Zhongyang, N. Mingjiang, C. Kefa, Mercury oxidation over
402 a vanadia-based selective catalytic reduction catalyst, *Energy and Fuels.* 23 (2009) 253–259.

- 403 [26] S. Xiong, J. Chen, N. Huang, T. Yam, Y. Peng, J. Li, The poisoning mechanism of gaseous HCl
404 on low-temperature SCR catalysts: MnO_x-CeO₂ as an example, *Appl. Catal. B Environ.* 267 (2020)
405 118668.
- 406 [27] A. S. Negreira, J. Wilcox, DFT Study of Hg Oxidation across Vanadia-Titania SCR Catalyst
407 under Flue Gas Conditions, *J. Phys. Chem. C.* 117 (2013) 1761-1772.
- 408 [28] K. Alexopoulos, P. Hejduk, M. Witko, M.-F. Reyniers, G. B. Marin, Theoretical Study of the
409 Effect of (001) TiO₂ Anatase Support on V₂O₅, *J. Phys. Chem. C.* 114 (2010) 3115-3130.
- 410 [29] B. Zhang, J. Liu, G. Dai, M. Chang, C. Zheng, Insights into the mechanism of heterogeneous
411 mercury oxidation by HCl over V₂O₅/TiO₂ catalyst: Periodic density functional theory study, *Proc.*
412 *Combust. Inst.* 35 (2015) 2855–2865.
- 413 [30] Y. Gao, Z. Li, A DFT study of the Hg⁰ oxidation mechanism of the V₂O₅-TiO₂ (001) surface,
414 *Mol. Catal.* 433 (2017) 372-382.
- 415 [31] L. Zhao, Y. Liu, Y. wen Wu, J. Han, S. lin Zhang, Q. Lu, Y. ping Yang, Mechanism of
416 heterogeneous mercury oxidation by HCl on V₂O₅(001) surface, *Curr. Appl. Phys.* 18 (2018) 626–
417 632.
- 418 [32] Y.-W. Wu, Z. Ali, Q. Lu, J. Liu, M.-X. Xu, L. Zhao, Y.-P. Yang, Effect of WO₃ doping on the
419 mechanism of mercury oxidation by HCl over V₂O₅/TiO₂ (001) surface: Periodic density functional
420 theory study, *Appl. Surf. Sci.* 487 (2019) 369-378.
- 421 [33] N. Usberti, S. Alcove Clave, M. Nash, A. Beretta, Kinetics of Hg⁰ oxidation over a
422 V₂O₅/MoO₃/TiO₂ catalyst: Experimental and modelling study under DeNO_x inactive conditions,
423 *Appl. Catal. B: Environ.* 193 (2016) 121-132.
- 424 [34] M. Koebel, M. Elsener, M. Kleemann, Urea-SCR: a promising technique to reduce NO_x
425 emissions from automotive diesel engines, *Catal. Today.* 59 (2000) 335–345.
- 426 [35] M. Koebel, M. Elsener, G. Madia, Reaction pathways in the selective catalytic reduction process
427 with NO and NO₂ AT low temperatures, *Ind. Eng. Chem. Res.* 40 (2001) 52–59.
- 428 [36] G. Madia, M. Koebel, M. Elsener, A. Wokaun, The effect of an oxidation on the NO_x reduction
429 by ammonia SCR, *Ind. Eng. Chem. Res.* 41 (2002) 3512–3517.

- 430 [37] M. Koebel, G. Madia, F. Raimondi, A. Wokaun, Enhanced reoxidation of Vanadia by NO₂ in
431 the fast SCR Reaction, *J. Catal.* 209 (2002) 159–165.
- 432 [38] L. Arnason, H. Falsig, S. B. Rasmussen, J. V. Lauritsen, P. G. Moses, A complete reaction
433 mechanism for standard and fast selective catalytic reduction of nitrogen on low coverage VO_x/TiO₂(
434 0 0 1) catalysts. *J. Catal.* 346 (2017) 188-197.
- 435 [39] N.-Y. Topsøe, Mechanism of the Selective Catalytic Reduction of Nitric Oxide by Ammonia
436 Elucidated by in Situ On-Line Fourier Transform Infrared Spectroscopy. *Science.* 265 (5176) (1994)
437 1217.
- 438 [40] E. Tronconi, I. Nova, D. Ciardelli, M. Chatterjee, M. Weibel, Redox features in the catalytic
439 mechanism of the “standard” and “fast” NH₃-SCR of NO_x over a V-based catalyst investigated by
440 dynamic methods. *J. Catal.* 245 (2007) 1-10.
- 441 [41] T. H. Vuong, J. Radnik, J. Rabeah, U. Bentrup, M. Schneider, H. Atia, U. Armbruster, W.
442 Grünert, A. Brückner, Efficient VO_x/Ce_{1-x}Ti_xO₂ Catalysts for Low-Temperature NH₃-SCR Reaction
443 Mechanism and Active Sites Assessed by in Situ/Operando Spectroscopy, *ACS Catal.* 7 (2017) 1693-
444 1705.
- 445 [42] Y. Peng, C. Wang, J. Li, Structure-activity relationship of VO_x/CeO₂ nanorod for NO removal
446 with ammonia, *Appl. Catal. B Environ.* 144 (2014) 538-546.
- 447 [43] L. Chen, J. Li, M. Ge, Promotional Effect of Ce-doped V₂O₅-WO₃/TiO₂ with Low Vanadium
448 Loadings for Selective Catalytic Reduction of NO_x by NH₃, *J. Phys. Chem. C.* 113 (2009), 21177-
449 21184.
- 450 [44] Z. Liu, S. Zhang, J. Li, L. Ma, Promoting effect of MoO₃ on the NO_x reduction by NH₃ over
451 CeO₂/TiO₂ catalyst studied with in situ DRIFTS, *Appl. Catal. B Environ.* 144 (2014) 90-95.
- 452 [45] A. Marberger, D. Ferri, M. Elsener, A. Sagar, C. Artner, K. Scherzanz, O. Kröcher, Relationship
453 between structures and activities of supported metal vanadates for the selective catalytic reduction of
454 NO by NH₃, *Appl. Catal. B Environ.* 218 (2017) 731-742.
- 455 [46] P. A. Kumar, Y. E. Jeong, H. P. Ha, Low temperature NH₃-SCR activity enhancement of
456 antimony promoted vanadia-ceria catalyst, *Catal. Today.* 293-294 (2017) 61-72.

- 457 [47] W. Hu, Y. Zhang, S. Liu, C. Zheng, X. Gao, I. Nova, E. Tronconi, Improvement in activity and
458 alkali resistance of a novel V-Ce(SO₄)₂/Ti catalyst for selective catalytic reduction of NO with NH₃,
459 Appl. Catal. B Environ. 206 (2017) 449-460.
- 460 [48] S. Gillot, G. Tricot, H. Vezin, J-P. Dacquin, C. Dujardin, P. Granger, Development of stable and
461 efficient CeVO₄ system for the selective reduction of NO_x by ammonia: Structure-activity
462 relationship, Appl. Catal. B Environ. 218 (2017) 338-348.
- 463 [49] A. Porta, T. Pellegrinelli, L. Castoldi, R. Matarrese, S. Morandi, S. Dzwigaj, L. Lietti, Low
464 Temperature NO_x Adsorption Study on Pd-Promoted Zeolites, Top. Catal. 61 (2018) 2021-2034.
- 465 [50] R. Willi, B. Roduit, R.A. Koepfel, A. Wokaun, A. Baiker, Selective reduction of NO by
466 NH₃ over vanadia-based commercial catalyst: Parametric sensitivity and kinetic modelling, Chem.
467 Eng. Sci. 51 (11) (1996), 2897-2902.
- 468 [51] B. Roduit, A. Wokaun, A. Baiker, Global kinetic modeling of reactions occurring during
469 selective catalytic reduction of NO by NH₃ over Vanadia/Titania-based catalysts, Ind. Eng. Chem.
470 Res. 37 (12) (1998) 4577-4590.
- 471 [52] A. Marberger, D. Ferri, M. Elsener, O. Kröcher, The Significance of Lewis Acid Sites for the
472 Selective Catalytic Reduction of Nitric Oxide on Vanadium-Based Catalysts, Angew. Chemie - Int.
473 Ed. 55 (2016) 11989–11994.
- 474 [53] K. Hadjivanov, H. Knozinger, Species Formed after NO adsorption and NO+O₂ Co-adsorption
475 on TiO₂: an FTIR Spectroscopic Study, Phys. Chem. Chem. Phys. 2 (2000) 2803-2806.
- 476 [54] M. A. Larrubia, G. Ramis, G. Busca, An FT-IR study of the adsorption of urea and ammonia
477 over V₂O₅-MoO₃-TiO₂ SCR catalysts, Appl. Catal. B. Environ. 27 (3) (2000) L145-L151.
- 478 [55] T.J. Dines, C.H. Rochester, A.M. Ward, Infrared and Raman study of the adsorption of nitrogen
479 oxides on titania-supported vanadia catalysts, J. Chem. Soc. Faraday Trans. 87 (1991) 1617–1622.
- 480 [56] R. Mikhaylov, A.A. Lisachenko, B.N. Shelimov, V.B. Kazansky, G. Martra, S. Coluccia, FTIR
481 and TPD Study of the Room Temperature Interaction of a NO-Oxygen Mixture and of NO₂ with
482 Titanium Dioxide, J. Phys. Chem. C. 117 (20) (2013) 10345-10352.

- 483 [57] D.E. Doronkin, F. Benzi, L. Zheng, D.I. Sharapa, L. Amidani, F. Studt, P.W. Roesky, M. Casapu,
484 O. Deutschmann, J-D. Grunwaldt, NH₃-SCR over V-W/TiO₂ Investigated by Operando X-ray
485 Absorption and Emission Spectroscopy. *J. Phys. Chem. C.* 123 (23) (2019) 14338-14349.
- 486 [58] R. Kuma, T. Kitano, T. Tsujiguchi, T. Tanaka, In Situ XANES Characterization of V₂O₅/TiO₂-
487 SiO₂-MoO₃ Catalyst for Selective Catalytic Reduction of NO by NH₃, *Ind. Eng. Chem. Res.* 59 (30)
488 (2020) 13467-13476.
- 489 [59] Y. Ganjkhanlou, T. V.W. Janssens, P. N.R. Vennestrøm, L. Mino, M. C. Paganini, M. Signorile,
490 S. Bordiga, G. Berlier, Location and activity of VO_x species on TiO₂ particles for NH₃-SCR catalysis,
491 *Appl. Catal. B: Environ.* 278 (2020) 119337.
- 492 [60] R. J. G. Niguide, D. Ferri, A. Marberger, M. Nachtegaal, O. Kroeche, Modulated Excitation
493 Raman Spectroscopy of V₂O₅/TiO₂: Mechanistic Insights into the Selective Catalytic Reduction of
494 NO with NH₃. *ACS Catal.* 9 (2019) 6814-6820.
- 495 [61] M. M. Mason, Z. R. Lee, M. Vasiliu, I. E. Wachs, D. A. Dixon, Initial Steps in the Selective
496 Catalytic Reduction of NO with NH₃ by TiO₂-Supported Vanadium Oxides, *ACS Catal.* 10 (2020)
497 13918-13931.
- 498 [62] W. Hu, R. Zou, Y. Dong, S. Zhang, H. Song, S. Liu, C. Zheng, I. Nova, E. Tronconi, X. Gao,
499 Synergy of vanadia and ceria in the reaction mechanism of low-temperature selective catalytic
500 reduction of NO_x by NH₃. *J. Catal.* 391 (2020) 145-154.

501

502

503

504

505

506

507

508 **Captions**

509 **Figure 1** – NO conversion in NH₃-SCR activity tests over HCl-doped catalyst (120 mg). Total flow
510 rate = 236 Nml/min. Composition: 300 ppm NO, 320 ppm NH₃, 3% O₂, balance He. Temperature
511 ramp = 5°C/min up to 400°C; 3.5 h hold at 400°C.

512 **Figure 2** – NO conversion during NO+O₂-TPSR after NH₃ saturation on HCl-doped V/Mo/Ti catalyst
513 (two consecutive experiments) and undoped catalyst. Catalyst = 80 mg. Total flow rate = 200
514 Nml/min. Composition: 100 ppm NO, 1000 ppm O₂ in He. T-ramp = 5°C/min.

515 **Figure 3** – NO concentration during the temperature ramp, after 2 hours adsorption at 100°C. Catalyst
516 = 200 mg, total flow = 200 Nml/min. Composition: 100 ppm NO, 1000 ppm O₂. Temperature ramp
517 = 5°C/min.

518 **Figure 4** – Differential FTIR spectra collected under flowing NO+O₂ at 25°C. (a) undoped catalyst,
519 2% V/TiO₂; (b) HCl-doped catalyst, 2% V/TiO₂. Composition: 1000 ppm NO, 3% O₂ in He. The insert
520 shows the 2000-2100 cm⁻¹ wavenumber range.

521

522

523

524

525

526

527

528

529

530

531

532

533

534

535

536

537

538

539

540

541

542

Figures

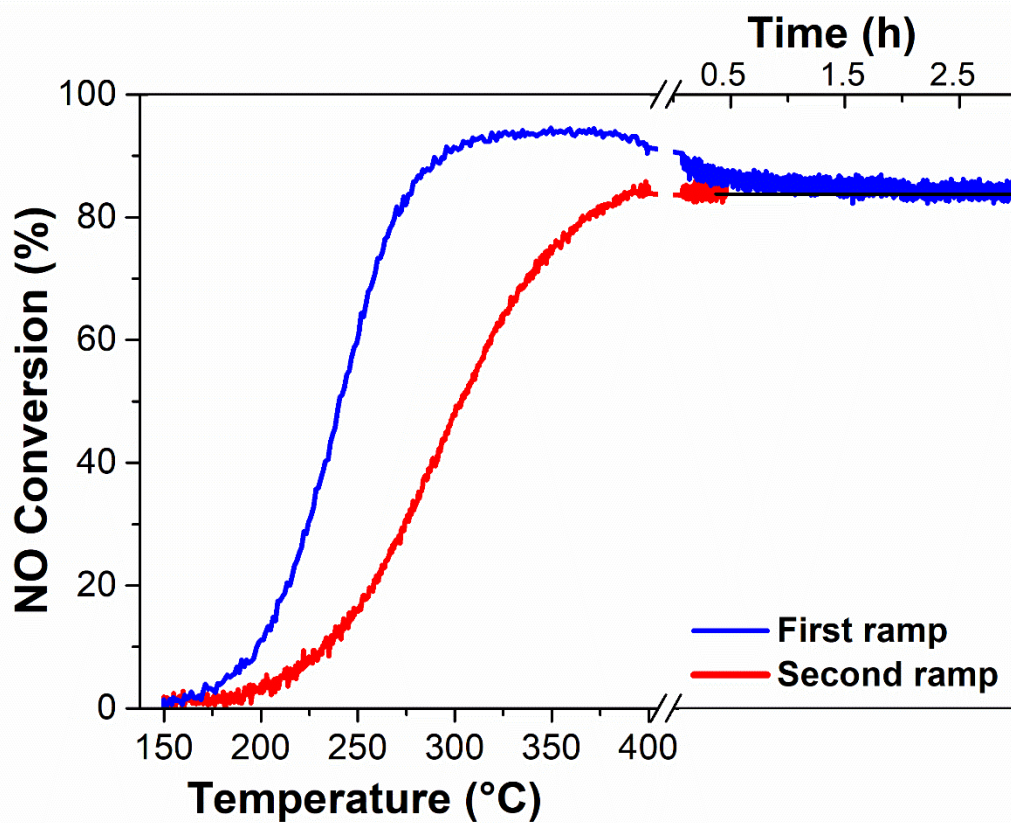
543

544

545

[Figure 1]

546



547

548

549

550

551

552

553

554

555

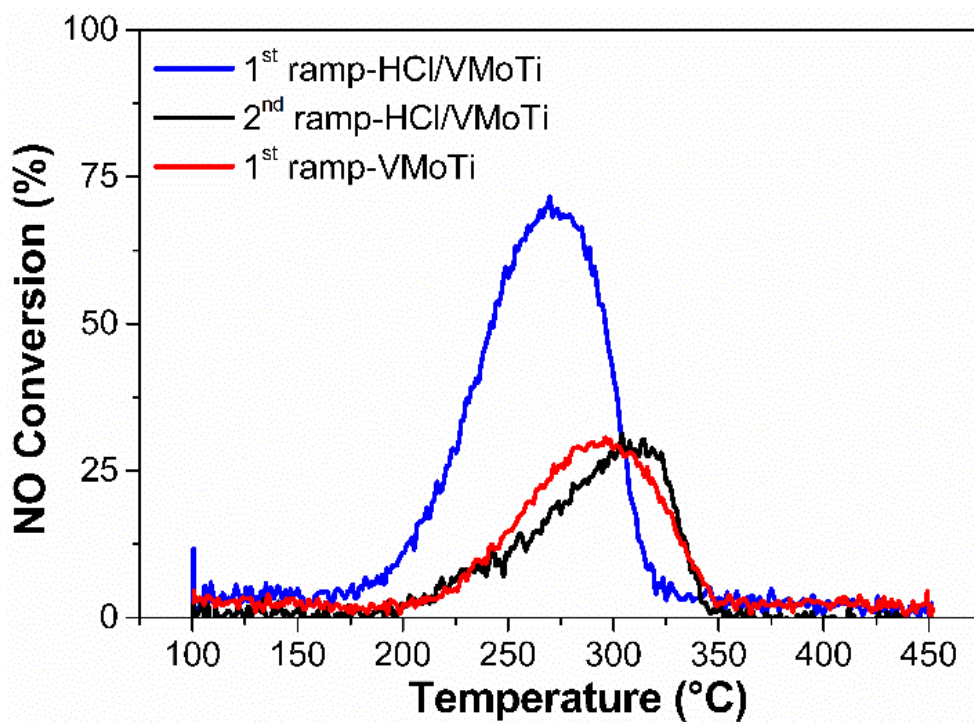
556

557

558

559

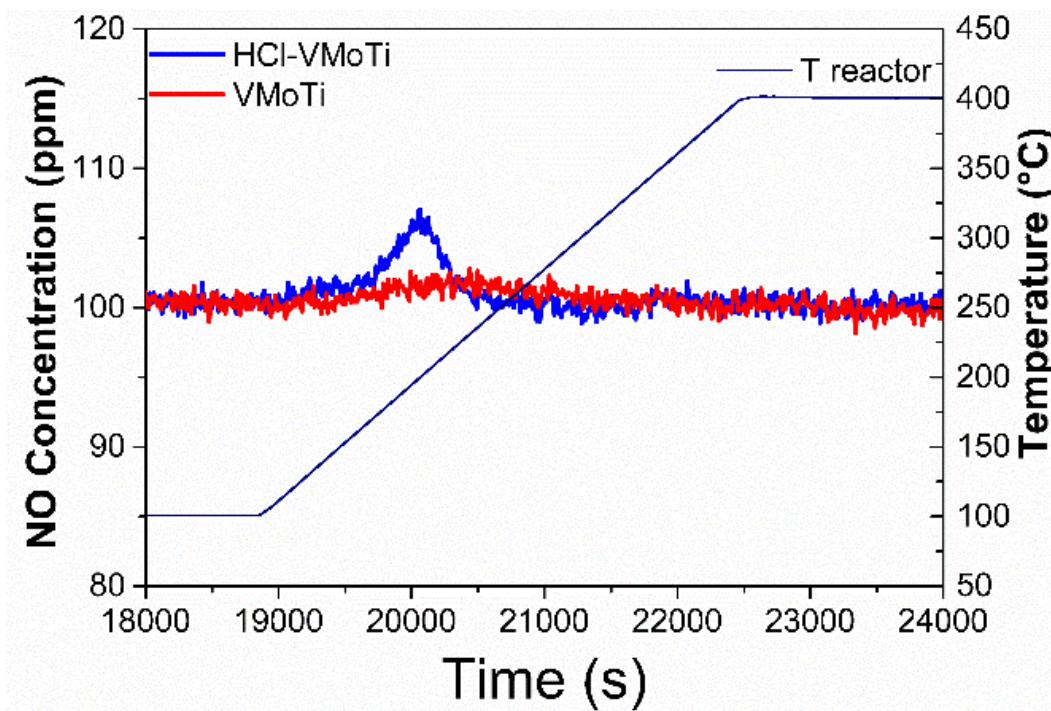
[Figure 2]



565
566
567
568
569
570
571
572
573
574
575
576
577
578
579
580
581

582
583
584
585
586
587

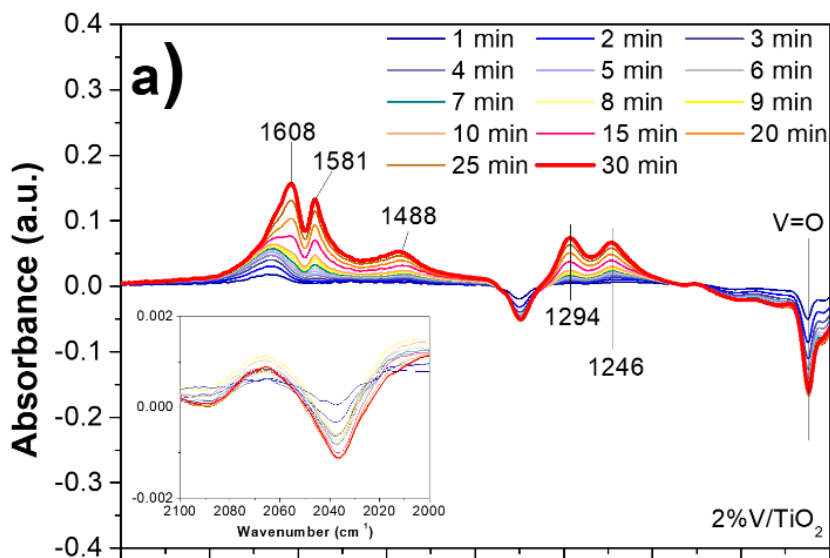
[Figure 3]



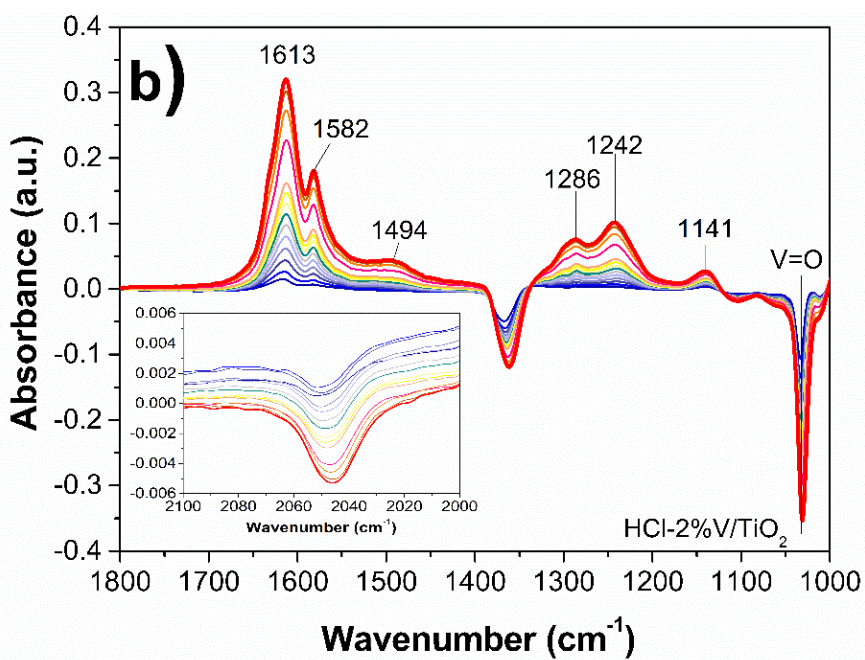
588
589
590
591
592
593
594
595
596
597
598
599
600
601
602
603

604
605
606
607
608

[Figure 4]



609
610



611
612
613
614
615
616

Supplementary Material

HCl-doping of V/TiO₂-based catalysts reveals the promotion of NH₃-SCR and the rate limiting role of NO oxidative activation

Aldo Lanza^a, Lei Zheng^{a,b}, Roberto Matarrese^a, Luca Lietti^a, Jan-Dierk Grunwaldt^b, Silvia Alcove Clave^c,
Jillian Collier^c, Alessandra Beretta^{a,*}

^a *Laboratory of Catalysis and Catalytic Processes, Dipartimento di Energia, Politecnico di Milano, via La Masa 34, 20156 Milano, Italy*

^b *Institute for Chemical Technology and Polymer Chemistry, Karlsruhe Institute of Technology, 76131 Karlsruhe, Germany*

^c *Johnson Matthey Technology Centre, Blounts Ct Rd, Sonning Common, Reading RG4 9NH, United Kingdom*

Key-words: NH₃-SCR, HCl, V₂O₅-MoO₃/TiO₂, NO activation, transient kinetic experiments, operando FT-IR

653 **Catalyst samples**

654 The commercial V₂O₅-MoO₃/TiO₂ is a JM proprietary catalyst used in several long-term applications
655 including coal-fired power plants, and combined biomass-coal power plants (with typically more than 10% of
656 water, 1-50 ppm of HCl).

657 The catalyst was received in the form of slabs cut from the commercial plates. The catalyst layer was
658 removed from the metal net, crushed and calcined in situ at 450°C under air flow of 200 Nml/min. The catalyst
659 was impregnated with HCl by Incipient Wetness Impregnation method with a solution of 2.31mol/l prepared
660 from a commercial concentrated HCl solution (37% solution in water, Acros Organics) and the resulting
661 powders were dried overnight at 110°C in oven. ICP analysis showed a content of Cl of 0.12-0.13% (w/w).
662 The catalyst with HCl is indicated in this work as “HCl-VMoTi”, while the reference catalyst as “VMoTi”.

663 A binary model catalyst 2%V/TiO₂ was prepared by IWI of TiO₂ (Tronox DT-51 anatase) with a
664 solution of ammonium metavanadate (NH₄VO₃), oxalic acid and water (stirred at 80°C to ensure the complete
665 dissolution of the salt). Impregnated powders were dried overnight at 100°C and calcined at 500°C for 2 h in
666 air. The HCl impregnation was obtained by applying the same procedure as the VMoTi catalyst. The binary
667 catalyst with HCl is indicated in this work as “HCl-2VTi”, while the reference catalyst as “2VTi”.

668

669 **SCR-Temperature-Programmed Reaction**

670 The reactivity of the HCl-VMoTi was tested by SCR-Temperature Programmed Reaction. The results
671 are reported in Figure 1. A fixed-bed quartz tubular reactor was prepared with 120 mg of HCl-VMoTi catalyst
672 (140-200 mesh) mixed with 180 mg quartz particles (same mesh).

673 The catalytic bed was dried for 60 min at 150°C under 3%O₂/He flow (236 Nml/min); afterwards, the
674 feed mixture (300 ppm NO, 320 ppm NH₃ 3% O₂ in He) was fed (236 Nml/min) for 60 min at 150°C. A
675 temperature ramp was then started from 150 to 400°C (5°C/min), with final hold of 3 h at 400°C. The reactor
676 was then cooled down to 150 °C under 3%O₂/He flow (236 Nml/min). A second ramp was finally started with
677 the same conditions as the first ramp.

678 The experimental set-up is equipped with an Online QMS Mass Spectrometer (Thermostar Pfeiffer
679 Vacuum) where signals of each reactant of interest are detected. Data are processed and elaborated to eliminate
680 drifts and cross-influences of the signals due to mass fragmentations, and to quantify the concentrations; to

681 this scope, calibration of the instrument is periodically repeated by means of calibration mixtures and
682 development of deconvolution algorithms.

683

684 **NO+O₂-Temperature-Programmed Surface Reaction over HCl-VMoTi and VMoTi**

685 For the NO+O₂-TPSR experiments, fixed-bed reactors were prepared with 80 mg of catalyst and 120
686 mg of quartz particles (140-200 mesh). The catalytic bed was initially dried under He flow (200 Nml/min) at
687 150°C. After drying, a flow of 500 ppm of NH₃/He was fed for NH₃ pre-adsorption for 90 min at 100°C; the
688 treatment was followed by a purge in He for 2h at 100°C.

689 A feed flow of NO=100 ppm and O₂=0.1% was then fed for 60 min at 100°C and a first ramp was set
690 from 100 to 450°C (5°C/min heating rate). The reactor was then cooled down to 100 °C under 0.1%O₂/He
691 flow (200 Nml/min) and the same procedure was repeated for a second experiment.

692

693 **NO+O₂ adsorption over HCl-VMoTi and VMoTi**

694 A fixed-bed quartz tubular reactor was prepared with 200 mg of catalyst mixed with 200 mg of quartz
695 powders (140-200 mesh) and was initially dried under He flow (200 Ncc/min) at 150°C. Then the catalyst was
696 cooled down to 100°C and NO=100 ppm + O₂=1000 ppm were fed with He as balance at the total flowrate of
697 200 Nml/min at 100°C for 2h. The temperature ramp was then started up to 400°C (5°C/min of heating rate),
698 keeping the NO+O₂ in He flow.

699

700 **SCR activity tests over HCl-VMoTi and VMoTi**

701 A fixed-bed quartz tubular reactor was prepared with 60 mg of catalyst mixed with 120 mg of quartz
702 powders (140-200 mesh). SCR activity tests were performed with a flowrate of 236 Nml/min by feeding
703 NH₃=320 ppm, NO=300 ppm, O₂=3% in He.

704

705 **SCR activity experiments over HCl-2%V/TiO₂ and 2%V/TiO₂**

706 A fixed-bed quartz tubular reactor was prepared with 33 mg of catalyst mixed with 300 mg of quartz
707 powders (140-200 mesh). SCR activity tests were performed with a flowrate of 325 Nml/min by feeding
708 NH₃=320 ppm, NO=300 ppm, O₂=3% in He.

709 **NO+O₂ and NH₃ adsorption over HCl-2%V/TiO₂ and 2%V/TiO₂ on Operando FT-IR**

710 For the Operando FT-IR analysis the catalysts in form of self-supported wafers (ca. 15 mg, diameter
 711 = 13 mm) were placed into an IR reactor cell (ISRI Infrared Reactor, Granger, IN, USA) connected to gas lines
 712 with gas mixing devices and mass flow controllers. All the experiments were performed under a total flow of
 713 50 Nml/min. The spectra were collected on a FT-IR Vertex 70 (Bruker, Billerica, MA, USA) with a spectral
 714 resolution of 4 cm⁻¹ and accumulating 64 scans using a MCT detector. The samples were pre-oxidized at
 715 350°C (O₂=3% v/v in He) for 90 minutes and then cooled down to 25°C. The NO_x storage experiments were
 716 performed with gas inlet stream of NO=1000 ppm + O₂=3% v/v in He, for 30 minutes. For ammonia
 717 adsorption, the same pre-oxidation treatment was performed, then the catalyst was exposed to a He flow with
 718 NH₃=500 ppm for 30 minutes. All the spectra are reported as difference spectra: the spectrum subtracted is
 719 always that recorded at ambient temperature after the pre-oxidation treatment.

720

721 **Packed bed reactor model**

722 *NO mass balance:*

723
$$\frac{dc_{NO}}{dw_{cat}} = -\eta_{DeNOx} \cdot R_{DeNOx} \cdot \frac{1}{\dot{Q}} \quad (S1)$$

724 *with the initial condition:* $c_{NO}|_{w_{cat}=0} = c_{NO,in} \quad (S2)$

725 With the rate expression:

726
$$R_{DeNOx} = k c_{NO} = \left[\frac{cm^3}{s g_{cat}} \right] \left[\frac{mol}{cm^3} \right] \quad (S3)$$

727 The effectiveness factor is defined as follows:

728
$$\eta_{DeNOx} = \frac{1}{3 \cdot \Phi^2} \cdot (3 \cdot \Phi \cdot \coth(3 \cdot \Phi) - 1) \quad (S4)$$

729 The Thiele modulus is calculated with a pseudo first order kinetic:

730
$$\Phi_{DeNOx} = \frac{d_p[cm]}{6} \cdot \sqrt{\frac{k \rho}{D_{eff,NO}}} \quad (S5)$$

731

732 In Eq. (S1-S5), $\dot{Q} \left[\frac{cm^3}{s} \right]$ is total flow rate under actual T, P conditions, $k \left[\frac{cm^3}{s g_{cat}} \right]$ is the pseudo-first
 733 order activity constant, $C_{NO} \left[\frac{mol}{cm^3} \right]$ is the concentration of NO, $W_{cat} [g]$ is the catalyst weight, $D_{eff,NO} \left[\frac{cm^2}{s} \right]$
 734 is the effective intraporous diffusivity of NO, calculated as in reference [S2].

735 In this work, the model was applied to the estimates of the intrinsic rate constants of the catalyst
736 samples (with and without HCl). The model fit involved the data reported in Figure 1 (flow of NO, NH₃ and
737 O₂ in He with temperature ramp) and Figure 2 (NO+O₂ – TPSR) in the low temperature range. Although the
738 model is steady state, it can be suitably applied also to dynamic data when obtained under quasi-stationary
739 conditions as in the present case (temperature ramp of 5°C/min). The effectiveness factor was unitary under
740 the conditions analyzed.

741 The model fit has been herein reported in the form of Arrhenius plots, a conventional form of
742 representation of the measured and estimated intrinsic rate constant k (obtained by integration of Eq. S1)

$$743 \quad k = -\ln(1 - \chi_{NO}) \frac{Q(T)}{W} \quad (S6)$$

744 in a $\ln(k)$ vs $1/T$ plot that highlights the temperature sensitivity:

$$745 \quad \ln(k) = \ln(k_0) - \frac{E_{act}}{R} \cdot \frac{1}{T} \quad (S7)$$

746 We note that the use of this methodology becomes improper when the behavior of the reactor is
747 influenced (possibly limited) by the input/output dynamics; in particular the Arrhenius plots of dynamic data
748 obtained at high heating ramping rate can be highly misleading.

749
750 Additionally, the model was used to extrapolate the low-temperature quasi steady state behavior to
751 high temperature conditions, which better emphasizes where the deviations of the reactor behavior from the
752 stationary conditions prevailed.

753 The model application is exemplified in Figure S6b, where dashed lines are the calculated results
754 (extrapolated also to the higher temperature) and symbols are the experimental results.

755 The verifications confirmed that both for the HCl-doped and the undoped catalyst, the effectiveness
756 factor was equal to 1 within the experimental range, being 0.98 at 325°C for the very active HCl-doped catalyst.

757

758

759

760

761

Supplementary Figures

[Figure S1]

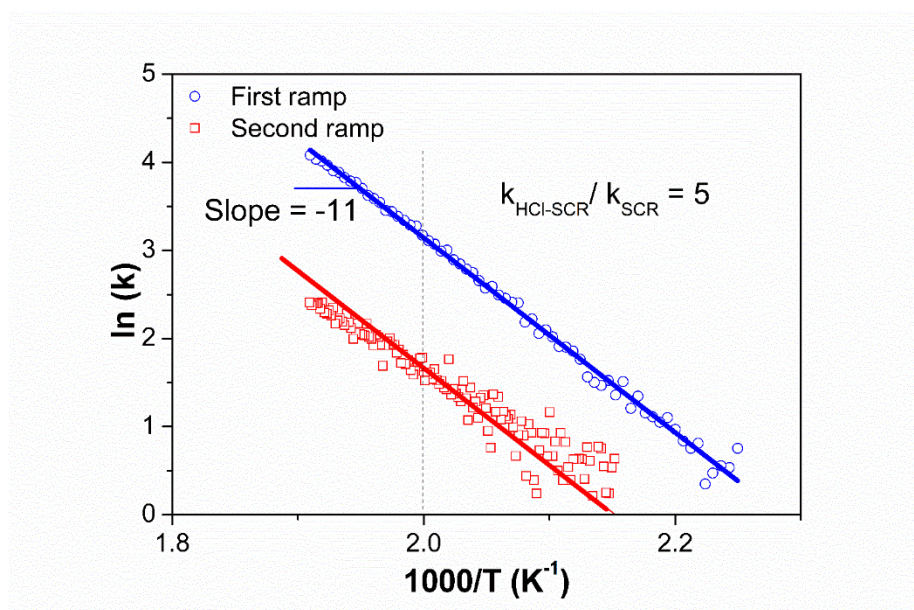
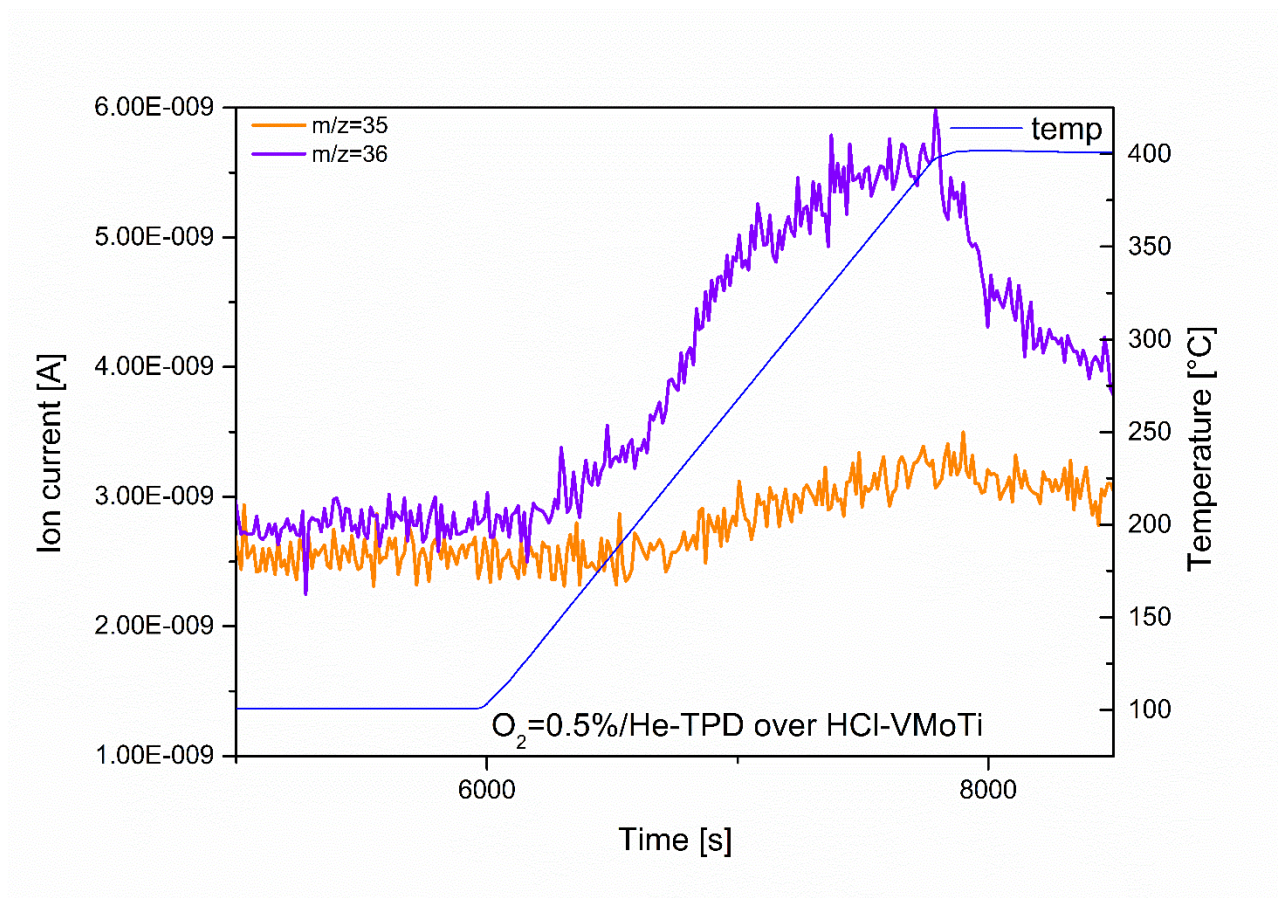


Figure S1 - Arrhenius plot of SCR-Temperature-programmed Reaction of Figure 1.

785

[Figure S2]



786

787

788 **Figure S2** – TPD over HCl-VMoTi catalyst (200 mg). Stabilization at 100°C, then ramp from 100
789 to 400°C (5°C/min). Total flow rate = 200 Nml/min. Composition: 0.5% O₂, balance He.

790

791

792

793

794

795

796

797

798

799

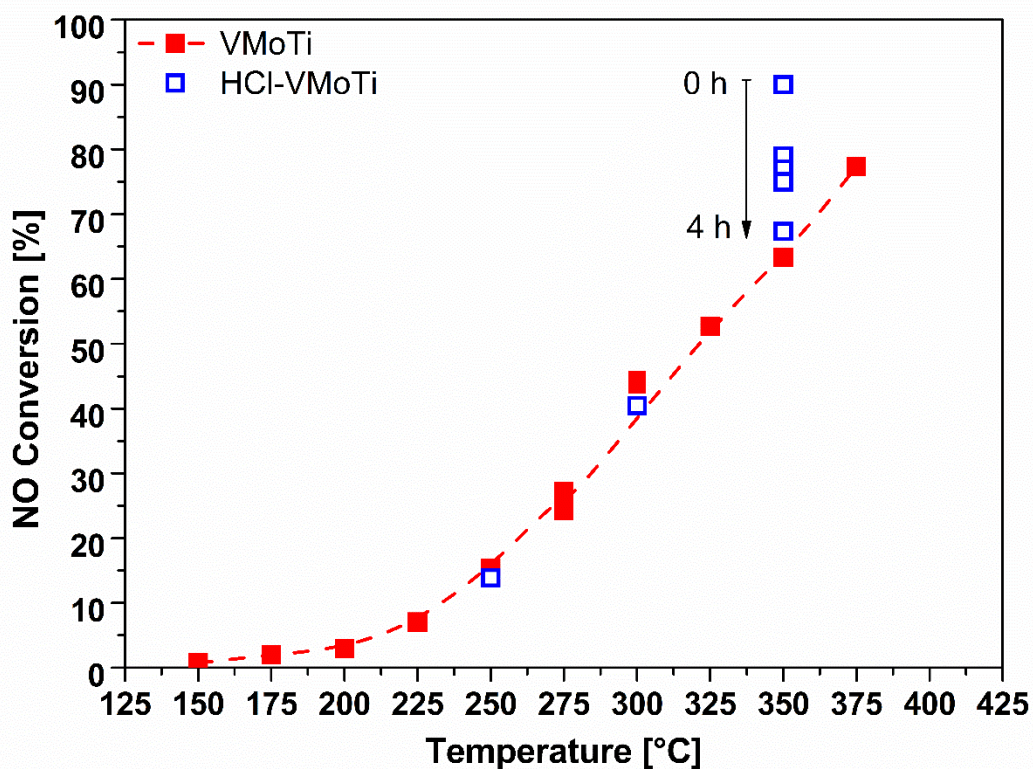
800

801

802

803
804
805
806
807
808

[Figure S3]

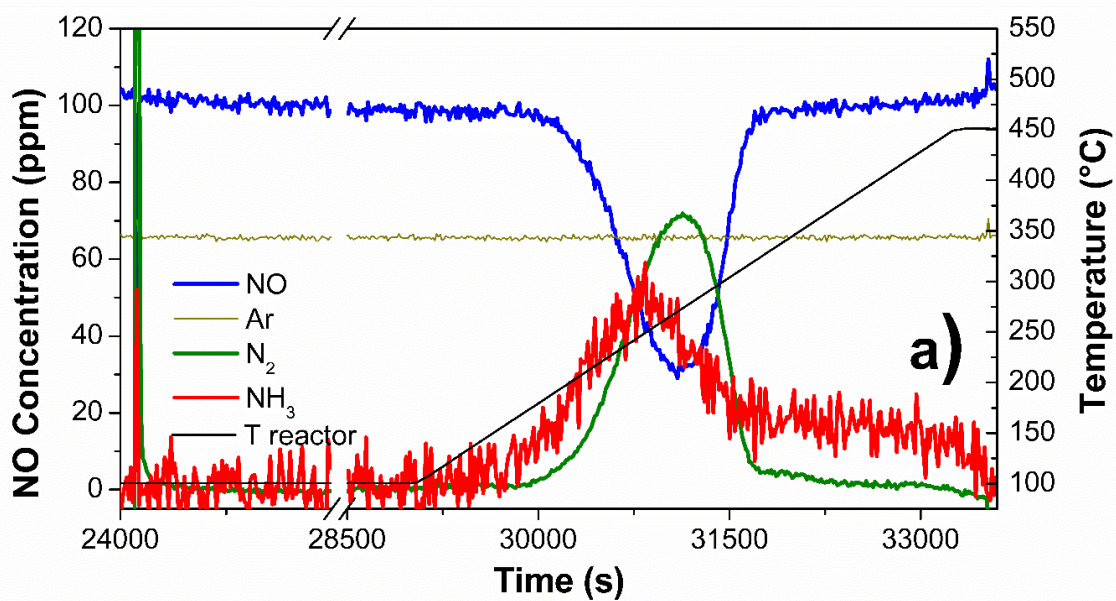


809
810

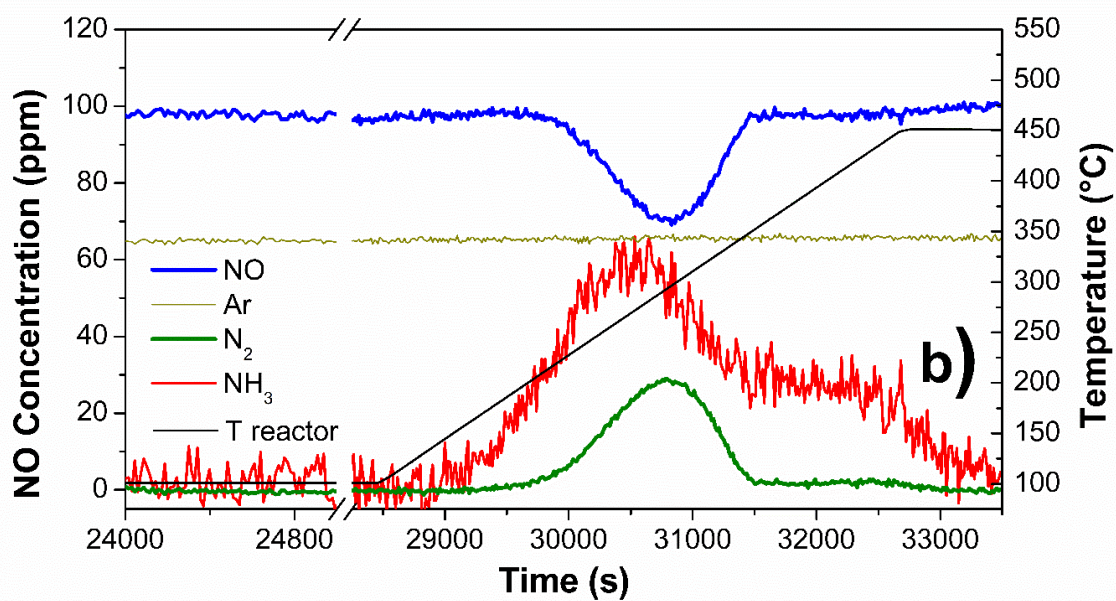
Figure S3 – NO conversion in NH₃-SCR steady state activity tests over HCl-doped catalyst (blue void squares, 60 mg) and over undoped catalyst (red squares, 60 mg). Total flow rate = 236 Nml/min. Composition: 300 ppm NO, 320 ppm NH₃, 3% O₂, balance He.

814
815
816
817
818
819

[Figure S4]



820



821

822

823

824

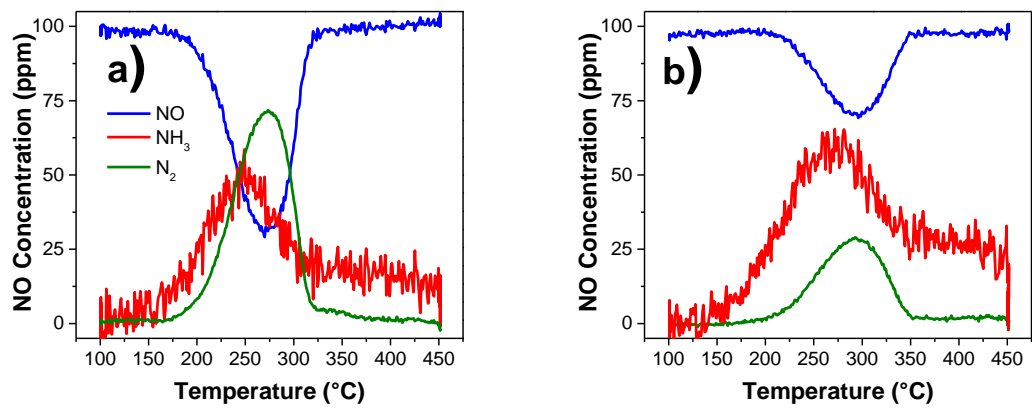
825 **Figure S4** - First run of NO+O₂-TPSR over a) HCl-VMoTi; first run of NO+O₂-TPSR over b)
 826 undoped VMoTi.

827

828

829

[Figure S5]



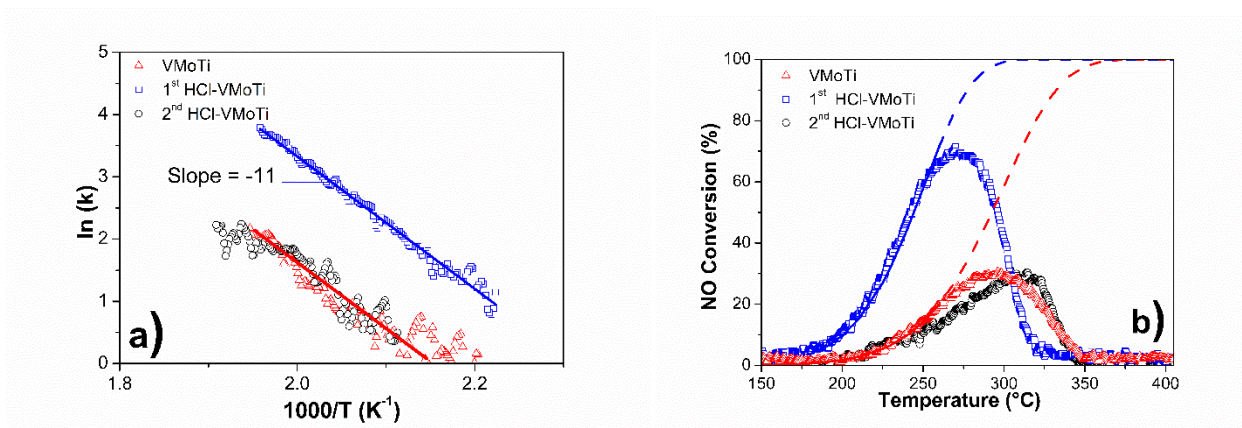
830
831
832
833
834

835 **Figure S5** - NO+O₂-TPSR versus temperature of the a) first run over HCl-VMoTi; b) First run over
836 undoped VMoTi

837
838
839
840
841
842
843
844
845
846
847
848
849
850
851
852
853
854
855
856
857

858
859
860

[Figure S6]



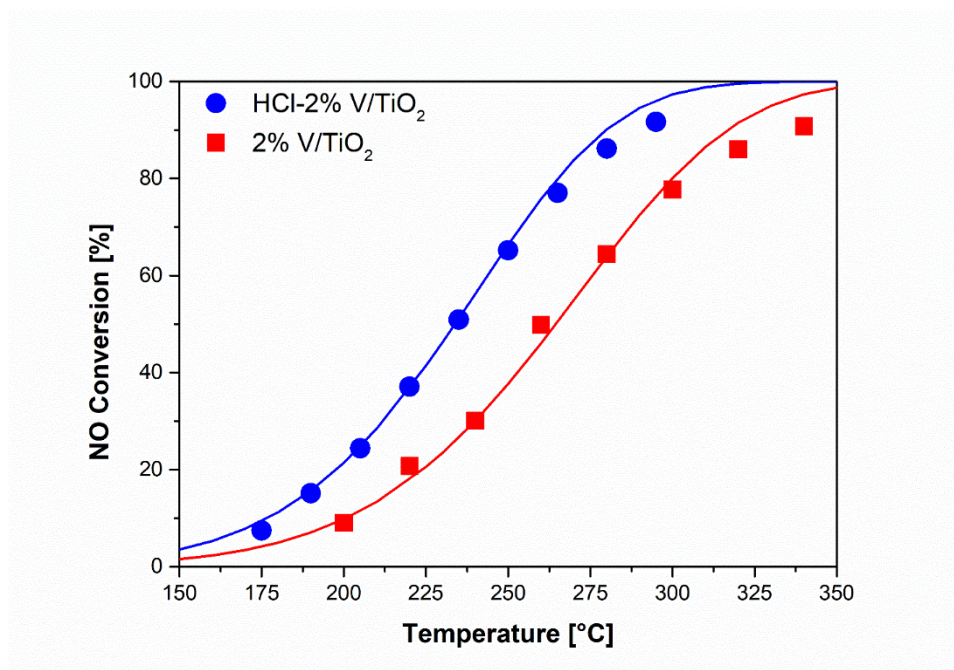
861
862
863
864
865

866 **Figure S6** - a) Arrhenius plot of NO+O₂-TPSR; b) Comparison between the prediction of a steady-
867 state reactor model with the results of the NO+O₂-TPSR. The model incorporates the intrinsic rate
868 constants obtained for both HCl-VMoTi and VMoTi within the range of temperature of 150-250 $^{\circ}C$:
869 $k_{VMoTi} = 12 \exp(-22000/RT (1/T-1/523.15))$ and $k_{HCl-VMoTi} = 68 \exp(-22000/RT (1/T-1/523.15))$

870
871
872
873
874
875
876
877
878
879
880
881
882
883

884
885
886

[Figure S7]



887
888
889

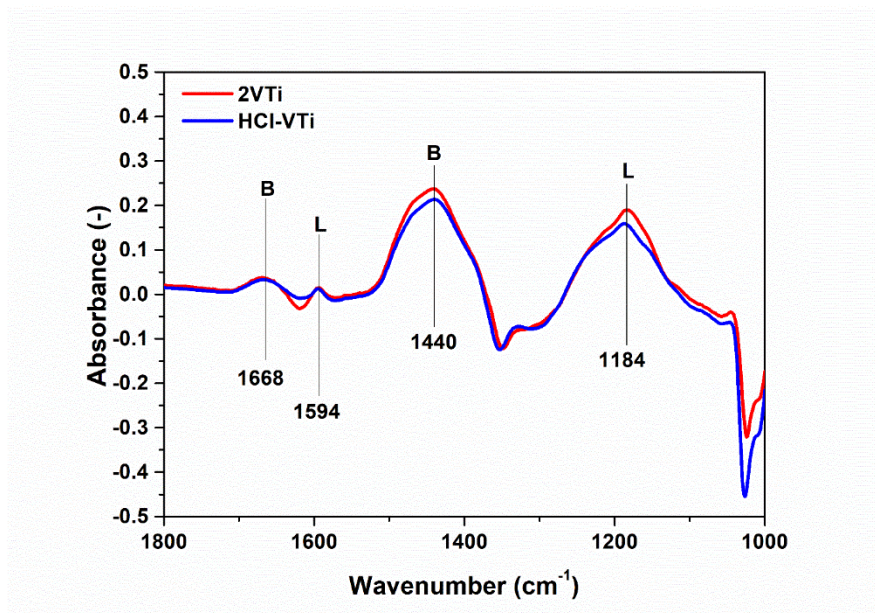
890 **Figure S7** – NO conversion in NH₃-SCR activity tests over 2% V/TiO₂ and impregnated HCl-
891 2% V/TiO₂ (33 mg). Total flow rate = 325 Nml/min. Composition: 300 ppm NO, 320 ppm NH₃, 3%
892 O₂, balance He.

893 The interpolating lines represent the result of a modelling analysis which allowed to evaluate the
894 intrinsic rate constants of the 2% VTi and the HCl-2% VTi catalysts: $k_{VTi} = 150 \exp(-16000/RT (1/T-$
895 $1/523.15))$ and $k_{HCl-VTi} = 350 \exp(-16000/RT (1/T-1/523.15))$.

896
897
898
899
900
901
902
903
904
905

906
907
908
909
910

[Figure S8]



911
912

913 **Figure S8** – Operando FT-IR spectra collected after 30 min at 25°C under NH₃=500 ppm/He over
914 2%V/TiO₂ and impregnated HCl-2%V/TiO₂. Total flowrate of 50 Nml/min.

915
916
917
918
919